Journal of Thermal Analysis and Calorimetry, Vol. 56 (1999) 969-982

THERMALLY STIMULATED CURRENT SPECTROSCOPY OF AMORPHOUS AND SEMI-CRYSTALLINE POLYMERS*

C. Bucharan, C. Dessaux, A. Bernès and C. Lacabanne

Laboratoire de Physique des Polymères, Université Paul Sabatier, 31062 Toulouse Cedex 04 France

Abstract

Thermally Stimulated Current (TSC) spectrometry has been applied to the characterization of polymeric materials. The study of a series of amorphous polymers having different physical structures has shown that the compensation parameters are independent of physical aging; contrarily, the activation enthalpy distribution reflects the evolution of the heterogeneity of the amorphous phase.

In copolymers, TSC allows us to identify segregated amorphous phases. In semi-crystalline polymers, with semi-rigid chains, we have shown the existence of an amorphous crystalline interphase characterized by a plateau in the temperature distribution of activation enthalpy.

Keywords: amorphous, dielectric relaxation, glass transition, polymer, structural relaxation, TSC spectrometry

Introduction

Polymeric materials always contain amorphous phases so that they are subjected to physical aging [1]. Since the corresponding structural evolution is responsible for significant modifications of macroscopic properties, a lot of work has been devoted to the characterization of physical aging. In classical studies, the return to equilibrium of the aged structure is analyzed by Differential Scanning Calorimetry (DSC) through the enthalpic relaxation. In the Tool-Narayanaswamy-Moynihan's model [2], the fictive temperature follows the structural evolution and the glassy state is defined by the limiting fictive temperature. Thus, the enthalpic relaxation is mainly characterized by its average activation enthalpy and by the parameter of the stretched exponential [2–5] deduced from the fictive temperature evolution.

Dielectric properties are widely dependent upon physical aging. The major effect concerns the main α dielectric relaxation of amorphous materials. Thermally Stimulated Currents (TSC) spectrometry has been applied to the analysis of this relaxation

* Plenary lecture.

1418–2874/99/ $ 5.00

Akadémiai Kiadó, Budapest

Kluwer Academic Publishers, Dordrecht

mode with a procedure analogous to DSC [6]. In other words, DSC and TSC experiments have been performed on samples having the analogous thermal history and so analogous physical structure. Consequently, complex TSC spectra can be compared with DSC curves. By using fractional polarizations, it is possible to determine, experimentally, the discrete distribution function of relaxation times associated to the α mode. Then, the evolution upon aging of parameters defining the temperature dependence of the relaxation times can be analyzed. The model polymer that has been chosen for this investigation is amorphous polyethylene terephthalate (PET).

Since TSC allows us to define amorphous phases, this technique can be applied to the analysis of phase segregation in multiphasic polymers. The example of a commercial copolymer – polyurethane – is given here in the second section of this paper. It is important to note here that the specific mechanical properties of this polymer are strongly dependent on phase segregation [7–11].

High modulus polymers are semi-crystalline. In this case, the mechanical strength is governed by the amorphous–crystalline interface–interphase. The third section of this paper is devoted to the investigation of this interface–interphase in semi-crystalline PET.

Experimental

Materials

Model samples used for this study were polyethylene terephthalate films – number average molecular mass $\overline{M}_n$=20000 g mol^{-1} –, kindly supplied by Rhône Poulenc (France). For the investigation of metastability and physical aging, a series of amorphous unoriented PET films were vitrified under various cooling rates q_c ranging from –0.5 to –50°C min^{-1}. For the analysis of amorphous crystalline interphase, bioriented semi-crystalline PET – 39% crystalline –, known as Terphane®, were used.

For the analysis of biphasic structures of amorphous polymers, a commercial amorphous polyurethane was used. Its formulation is based on diphenylmethane diisocyanate for hard segments, and on hydroxytelechelic polybutadiene for soft segments. The macrodiol has a mass average molecular mass comprise between 6000 and 7000 g mol^{-1}. The functionality is ranging between 2.15 and 2.38 [12, 13] giving a slightly crosslinked network. After bulk polymerization, all samples were cured at 80°C in an oven during one hour after 20 min under vacuum. Prior to the experiments, polyurethane samples were aged one year at room temperature.

Methods

Experimental studies of transitions were performed on a Differential Scanning Calorimeter DSC 7 with 10 to 14 mg samples enclosed in aluminium pans. The heating rate was 20°C min^{-1}. The thermal history of PET was previously erased by a 3 min annealing at 95°C.

TSC experiments were carried out on an experimental set up previously described [6]. Polymeric films were inserted in the condenser, under helium atmosphere. For the complex TSC spectra, the electrical field E was applied for 2 min at the polarization temperature T_p; then the samples were cooled at a rate q_c. Afterwards, E was switched off and the condenser was connected to the electrometer. A

controlled increase in temperature T at 7°C min^{-1} induced the return to equilibrium of the stored polarization. For facilitating comparative studies, the depolarization current density j was normalized to this applied electrical field. For fractional polarization (FP) experiments, the window was 5° and the increment of polarization temperature was also 5°.

Metastability and physical aging of amorphous polymers

Enthalpic relaxation

Thermoanalytical curves of heat capacity

Figure 1 shows the temperature dependence of heat capacity (ΔC_p) for glasses vitrified under cooling rates ranging from −0.5 to −50°C min^{-1}.

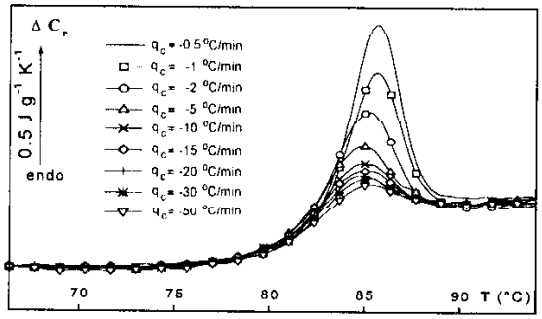

Fig. 1 DSC curves of amorphous PET vitrified under cooling rates q_c

DSC curves show the existence of two superimposed events:

→ the classical step of the glass transition T_g when the heat capacity is increasing from C_{pg} for $T \ll T_g$ till C_{pl} for $T \gg T_g$.

→ the endothermic peak reflecting enthalpic relaxation.

The magnitude of this peak is increasing when the absolute value of cooling rate decreases, that is to say when the physical aging level increases. It can be also seen that the maximum of this peak is shifted towards higher temperatures when the cooling rate is lower.

Temperature dependence of fictive temperature

An experimental variation of the fictive temperature T_f can be obtained from the following equation:

$$\int_{T_o}^{T_f}(C_{pl} - C_{pg})dT' = \int_{T_o}^{T}(C_p - C_{pg})dT' \qquad (1)$$

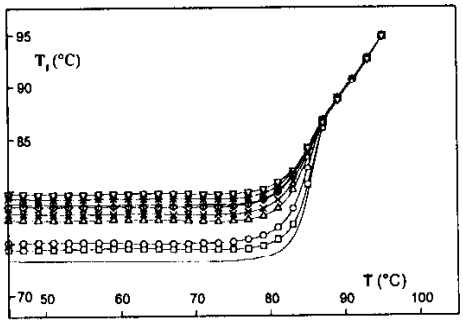

Fig. 2 Experimental fictive temperature as a function of temperature for amorphous PET vitrified under cooling rates indicated on Fig. 1

where T_0 is the starting temperature of the thermal cycle (in our case T_0=95°C), C_p is the heat capacity at temperature T, and T' is the running temperature. Figure 2 shows the experimental variation $T_f(T)$ evaluated from the experimental heat capacity reported on Fig. 1. It should be noted that, in the equilibrium state, well above T_g, the fictive temperature equals T. Well below T_g, the fictive temperature tends towards the limiting fictive temperature T_f' (T_f' is a characteristic of the glassy structure).

Analysis with a stretched exponential

For describing enthalpic relaxation, Moynihan *et al.* [2–5] have proposed to use a stretched exponential relaxation function:

$$\Phi(t) = \exp\left\{-\left(\frac{t}{\tau}\right)^{\beta}\right\} \tag{2}$$

where β represents the width of the relaxation function, and τ is the structure dependent relaxation time. Tool-Narayanaswamy-Moynihan have proposed for τ, the following equation:

$$\tau(T,T_f) = A\exp\left[x\frac{\Delta h^*}{RT} + (1-x)\frac{\Delta h^*}{RT_f}\right] \tag{3}$$

where x is a partitioning parameter defining the relative contribution of temperature and structure, Δh^* is the average activation enthalpy, A is a pre-exponential factor, and R is the gas constant.

Average activation enthalpy

The average activation enthalpy Δh^* is deduced separately from the slope of the plot of $\ln|q_c|$ *vs.* the reciprocal limiting fictive temperature T_f:

$$\frac{\mathrm{d}\ln|q_c|}{\mathrm{d}\left(\frac{1}{T_f'}\right)} = -\frac{\Delta h^*}{R} \tag{4}$$

The slope of the line defined by the experimental points gives $\Delta h^* \approx 650$ kJ mol^{-1}. It is interesting to note here that this value is in good agreement with the one obtained by Montserrat *et al.* [14].

β parameter of the stretched exponential

By matching the calculated and experimental values of dT_p/dT *vs.* T, we calculate the β parameter of the stretched exponential for the various cooling rates. β best fit parameters deduced in the range 0.5°C min$^{-1} \leq |q_c| \leq 50$°C min^{-1} are plotted as a function of $|q_c|$ on Fig. 3.

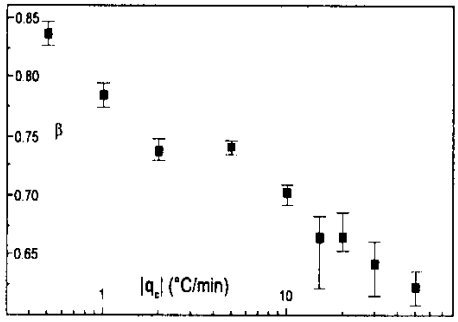

Fig. 3 β parameter of stretched exponential *vs.* $|q_c|$ for amorphous PET

The β parameter shows a marked increase as the absolute cooling rate decreases: β varies from 0.65 to 0.84 when $|q_c|$ varies from 50°C min^{-1} till 0.5°C min^{-1}. In other words, the width of the distribution function of the relaxation times decreases as physical aging increases. This result means that, for an infinitely slow cooling rate, β would tend towards 1 and the enthalpic relaxation would be monokinetic.

Dielectric relaxation

Complex TSC spectra

100 μm thick films were inserted in the condenser and subjected to a static field of 2.5 MV m^{-1} at T_p=80°C. Figure 4 shows the polarization recovery for the various cooling rates. A main TSC peak is observed at T_α: within an error of 1°C, $T_\alpha \approx T_g$ as determined by DSC. So, this α peak corresponds to the dielectric manifestation of the glass transition. The shape of this peak is evidently dependent upon the cooling rate: the lower the rate is, the steeper the peak. It is important to note here that this evolution is coherent first with the experimental variation of the heat capacity and second with the calculated β parameter.

Fine structure of TSC spectra

Complex TSC spectra can be experimentally resolved into elementary processes by using FP procedure [6]. So, the complex spectra will be described in the hypothesis of a discrete distribution of relaxation times. The explored temperature range is

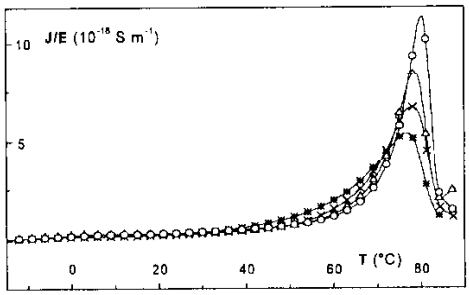

Fig. 4 Complex TSC spectra for amorphous PET vitrified under cooling rates indicated on Fig. 1

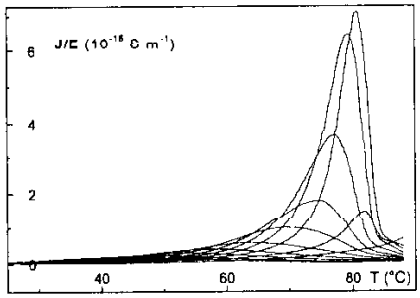

Fig. 5 Elementary TSC spectra for amorphous PET vitrified under q_c=−30°C min^{-1}

30 to 80°C. Figure 5 shows as an example the elementary spectra isolated for a cooling rate q_c=−30°C min^{-1}. The analysis of elementary spectra gives the temperature dependence of the corresponding relaxation times $\tau_i(T)$. According to the Bucci-Fieschi-Guidi analysis [15], each relaxation process has been characterized by an activated relaxation time $\tau_i(T)$:

$$\tau_i(T) = \frac{h}{k_b T}\exp\left(-\frac{\Delta S_i}{R}\right)\exp\left(\frac{\Delta H_i}{RT}\right) \tag{5}$$

where h is the Planck constant, k_b is the Boltzmann constant, ΔS_i is the activation entropy, and ΔH_i is the activation enthalpy.

Figure 6 shows the Arrhenius diagram of $\tau_i(T)$ for PET vitrified under a cooling rate of −30°C min^{-1}.

Compensation law

For any physical structure, we verify that the compensation law is obeyed i.e.:

$$\tau_i(T) = \tau_c \exp\left\{\frac{\Delta H_i}{R}\left(\frac{1}{T} - \frac{1}{T_c}\right)\right\} \tag{6}$$

where τ_c is the compensation time and T_c is the compensation temperature.

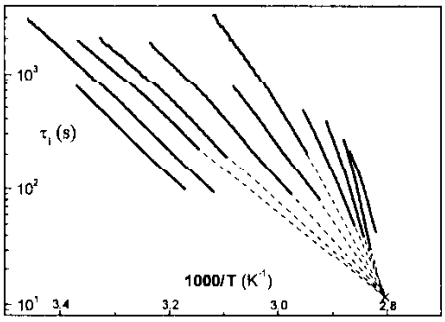

Fig. 6 Arrhenius diagram of amorphous PET vitrified under q_c= 30°C min^{-1}

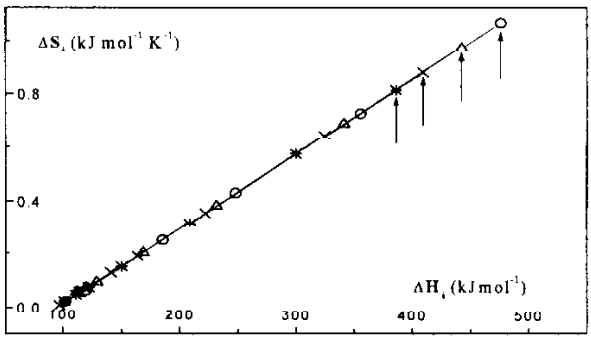

Fig. 7 Compensation diagram for amorphous PET vitrified under cooling rates indicated on Fig. 1

Equation (6) can be rewritten as:

$$\Delta S_i = \frac{\Delta H_i}{T_c} + \ln\left(\frac{h}{k_b T \tau_c}\right) \tag{7}$$

For the various cooling rates, ΔS_i has been plotted as a funciton of ΔH_i on a compensation diagram (Fig. 7). We obtain T_c=82°C and $\tau_c \approx 10$ s whatever the cooling rate is. The single compensation line confirms that T_c and τ_c are independent of physical aging. τ_c remains, as usual, of the order of seconds while $T_c \approx T_g$. Contrary to T_c and τ_c, the maximum activation enthalpy indicated by the arrows on Fig. 7, is characteristic of physical aging: indeed the maximum enthalpy increases with physical aging. This evolution is well illustrated by the temperature variation of the activation enthalpy (Fig. 8). This variation is of 89.7 kJ mol^{-1} for $|q_c|$ varying from 30 to 2°C min^{-1}. According to the Hoffman-Williams-Passaglia model [16], the activation parameters reflect the size of the mobile units. In other words, physical aging, is responsible for an increasing of the size of mobile units involved in cooperative movements liberated at T_g.

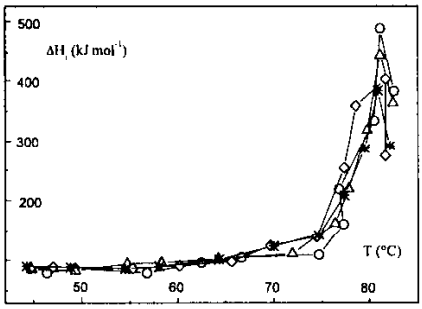

Fig. 8 Activation enthalpy *vs.* temperature for amorphous PET vitrified under cooling rates indicated on Fig. 1

Biphasic structure of amorphous polymers

Glass transition

Figure 9 shows the step obtained on polyurethane, between −100 and +130°C. We obtain a glass transition at −74°C and a specific heat jump of 0.028 J g^{-1} K^{-1}. This low glass transition temperature is characteristic of a segregated material. Like other authors [17, 18] we found for polyurethane a glass transition temperature near the polybutadiene glass transition temperature. It is the so called soft segments glass transition of polyurethane. This result is characteristic of phase segregation. Hard segments glass transition is not observed.

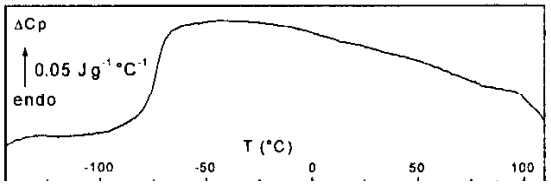

Fig. 9 DSC curves of polyurethane

Dielectric relaxation

Complex TSC spectra

1 mm thick samples were polarized by E=3 MV m^{-1} at T_p=80°C. The complex TSC spectra show a small peak at −80°C with a shoulder on the low-temperature side and a strong peak at 80°C (Fig. 10). Since the low-temperature peak is observed in the vicinity of the glass transition temperature of soft sequences, it has been attributed to the dielectric manifestation of the glass transition of soft sequences (SS). As for the high temperature peak, it might reflect the dielectric manifestation of the glass transition of hard sequences (HS). Above 100°C, the continuous current in-

crease has the characteristics of a Maxwell Wagner Sillars (MWS) polarization [19–21]. For ascertaining previous hypothesis, FP procedure has been applied.

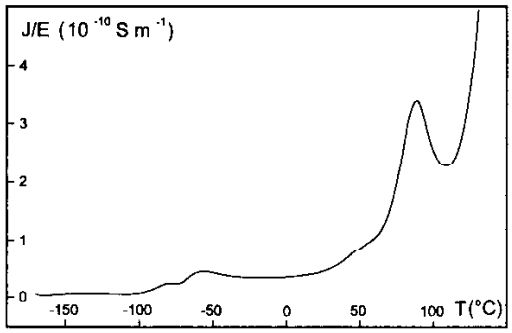

Fig. 10 Complex TSC spectra of polyurethane

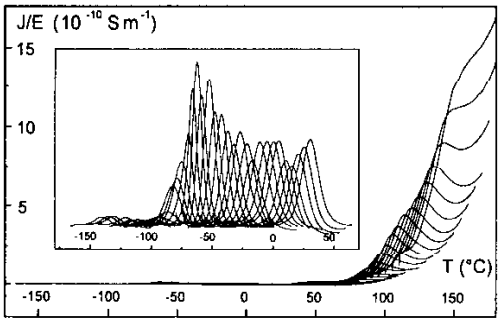

Fig. 11 Elementary TSC spectra of polyurethane

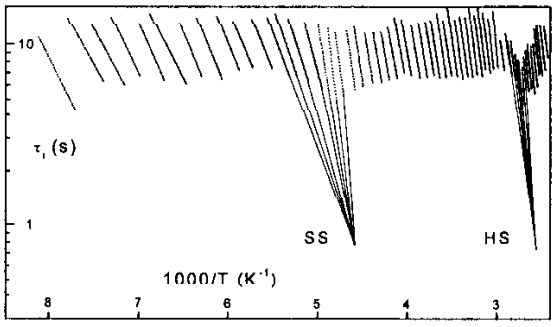

Fig. 12 Arrhenius diagram of polyurethane

Fine structure of TSC spectra

Figure 11 shows elementary TSC spectra of polyurethane. The analysis of the high-temperature peaks requires to subtract the MWS contribution. The Arrhenius diagram on Fig. 12 shows the existence of two compensation phenomena at, respectively, low-temperature (SS) and high temperature (HS). The compensation parameters defined by Eq. (6) are listed on Table 1. The two compensation phenomena correspond respectively, to the complex TSC peaks at −80 and +80°C. Since this behaviour is characteristic of the dielectric relaxation mode associated with T_g, it confirms the previous hypothesis.

Table 1 Compensation parameters for soft segments (SS) and hard segments (HS) of amorphous polyurethane

	T_c/°C	τ_c/s
SS	−55	0.58
HS	117	0.52

Activation parameters

The compensation diagram (Fig. 13) gives another representation of compensation phenomena. For the purpose of clarity, we have only reported, on this diagram, the experimental points corresponding to the elementary peaks isolated between −87 and 100°C. Each line is characteristic of the structure of one phase:

→ The line at lower enthalpies correspond to the phase constituted by soft sequences.

→ The line at higher enthalpies to the phase due to hard sequences.

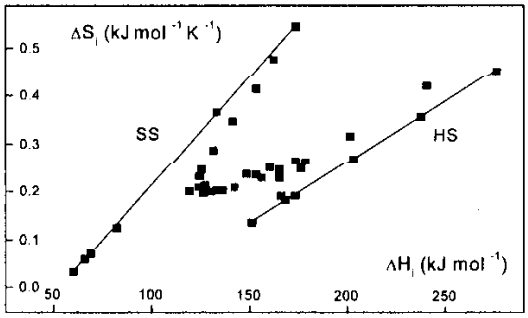

Fig. 13 Compensation diagram of polyurethane

Another manifestation of the biphasic structure is exhibited on the variation of activation enthalpy as a function of temperature (Fig. 14). Here, the enthalpy maxima are in the range of the glass transition. For the high-temperature peak, a precursor sub mode is observed.

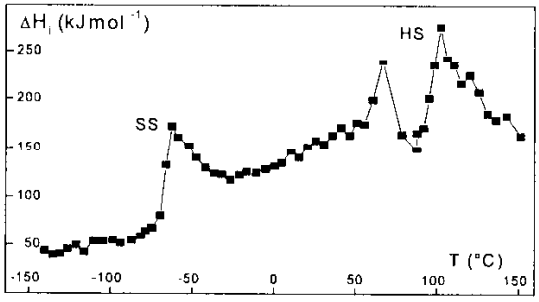

Fig. 14 Activation enthalpy *vs.* temperature for polyurethane

Amorphous–crystalline interphase in semi-crystalline polymers

Dielectric relaxation spectra

The complex TSC spectra of semi-crystalline PET have been recorded by using the same experimental procedure as involved in the amorphous PET one: the 10 MV m^{-1} electrical field was applied on 20 μm thick bi-oriented PET films for 2 min at the polarization temperature T_p=140°C and TSC spectra were recorded till 150°C. In order to erase the previous thermal history, the samples were annealed for 3 min at 140°C before the beginning of the next thermal history. The cooling rate values were about −70, −30, −10, −5 and −2°C min^{-1}, and the corresponding spectra are presented on Fig. 15. A peak located around 120°C is observed: whatever the cooling rate is, these peaks are well superimposed.

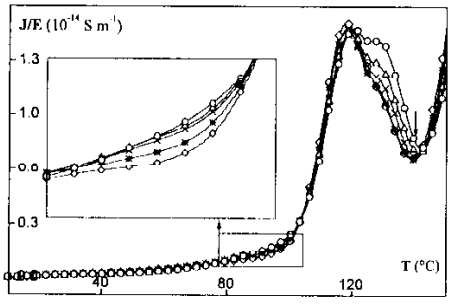

Fig. 15 Complex TSC spectra of semi-crystalline PET vitrified under the cooling rates indicated on Fig. 1. The diamond curve corresponds to the maximum experimental cooling rate (about −70°C min^{-1})

On the low-temperature side, when the absolute cooling rate decreases, we observe an evolution of the temperature dependent intensity (see cartoon). It reveals a peak around 80–100°C i.e. in the same temperature range that the TSC peak associ-

ated with the glass transition of amorphous PET. The upper temperature TSC peak located around 120°C is specific of semi-crystalline PET. So its origin would be related to the existence of crystallites. Note that, on the upper temperature side of this peak, we observe a shoulder located around 135°C. It is related to a weak modification of crystallinity ratio.

Activation enthalpy parameters

For isolating the elementary TSC spectra, FP procedure has been applied in the temperature range 50–140°C. The temperature dependence of the various $\tau_i(T)$ follows Eq. (5). For $T<110$°C, the activation parameters corresponding to the elementary processes isolated in the series of semi-crystalline PET vitrified under various cooling rates, are reported on the compensation diagram (Fig. 16). Whatever the physical structure is, the compensation law is obeyed. The values of the compensation parameters as a function of cooling rate are reported on Table 2.

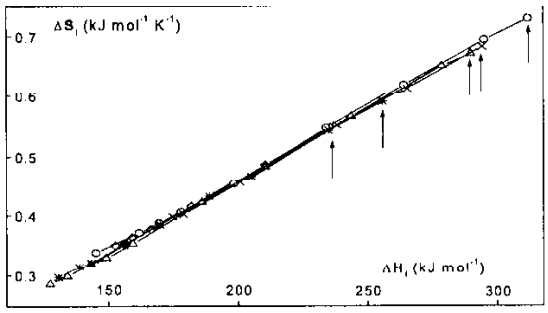

Fig. 16 Compensation diagram of semi-crystalline PET vitrified under cooling rates indicated on Fig. 15

Table 2 Compensation parameters of semi-crystalline PET

q_c/°C min^{-1}	~70	30	10	5	2
T_c/°C	136	144	140	133	137
τ_c/s	–0.9	–0.4	–0.3	–0.2	–0.2

Because of the analogy of behaviour with the mode observed in amorphous PET, this low-temperature mode has been assigned to the free amorphous phase i.e. free from interaction with crystallites.

The specific behaviour of semi-crystalline PET above 110°C is exhibited on the variation *vs.* temperature of activation enthalpy (Fig. 17). After the classical increase *vs.* temperature of ΔH_i for the low-temperature mode, a plateau is observed. It has been associated to a different zone: since this mobility is strongly dependent on the morphology of crystallites and chain rigidity, it has been assigned to amorphous regions constrained by crystallites. In fact, such a constrained amorphous phase constitutes the amorphous–crystalline interphase.

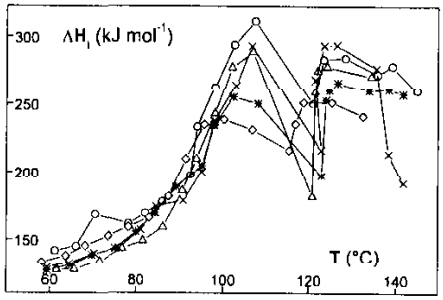

Fig. 17 Distribution of activation enthalpy of semi-crystalline PET vitrified under cooling rates indicated on Fig. 15

Discussion and conclusion

Metastability and physical aging of amorphous polymers have been characterized by analyzing enthalpic relaxation. With increasing physical aging, the limiting fictive temperature decreases while the β parameter of the stretched exponential increases. The influence of physical aging on dielectric relaxation of amorphous polymers has been analyzed with the model of discrete relaxation time. The evolution of dielectric relaxation has been found to be coherent with the one of enthalpic relaxation. The dielectric relaxation mode associated with the glass transition has been described by relaxation times following a compensation law. Compensation parameters are independent from physical aging. Contrarily, the maximum value of the activation enthalpy is increasing with physical aging reflecting an increasing of the size of mobile units. Since the size of mobile units reflects the size of domains where cooperative movements take place, this evolution is indicative of an increase of the heterogeneity of the amorphous phase of the polymer.

A wide variety of polymeric materials is biphasic. The polyurethane under investigation shows only one low-temperature glass transition in the range of the polybutadiene glass transition. The dielectric relaxation mode observed in the same temperature range is very weak. The dipole of the *cis* double bond responsible for the dielectric energy loss of polybutadiene is small [21], explaining the low magnitude of the corresponding TSC peak. The compensation law obeyed by the elementary processes constituting this mode is characteristic of the amorphous phase: τ_c is of the order of the second and $T_c \sim T_g + 20°C$. Such parameters are found in a wide variety of polymeric materials [23]. The dielectric relaxation mode observed at 80°C, has the same phenomenological behaviour than the preceding one. From the compensation parameters, we can predict a glass transition temperature around 97°C. The absence of step of heat capacity can be explained by the strongly polar character of this phase. The predicted T_g is coherent with values obtained on model hard segments by Cuvé *et al.* [24]. The existence of a well segregated biphasic structure explains the existence of a Maxwell Wagner Sillars effect at the boundary of the domains. It is interesting to note that this effect vanishes at a temperature (100°C) corresponding to the breaking of hydrogen bonds in hard domains of polyurethane as observed by IRTF spectroscopy [25].

Semi-crystalline polymers have been analyzed with the same procedure than amorphous polymers in order to facilitate comparative studies. Below 110°C, the same analytical behaviour as in amorphous polymers is observed, the compensation parameters are coherent while the maximum activation enthalpy increases upon physical aging.

Above 110°C, an intense peak specific of semi crystalline polymers is observed. It corresponds to a plateau in the distribution of activation enthalpy *vs.* temperature. This behaviour that has been observed in a wide series of semi-crystalline polymers with semi-rigid chains [23] has been attributed to the relaxation of amorphous sequences under stress from crystallites. Considering the influence of crystalline morphology and chain rigidity, this mode has been assigned to the amorphous–crystalline interphase of the polymer.

References

1 J. M. Hutchinson, Prog. Polym. Sci., 20 (1995) 703.
2 C. T. Moynihan, A. J. Easteal and M. A. Debolt, J. Am. Ceram. Soc., 59 (1976) 12.
3 C. T. Moynihan, P. B. Macedo, C. J. Montrose, P. K. Gupta, M. A. Debolt, J. F. Dill, B. E. Dom, P. W. Drake, A. J. Easteal, P. B. Elterman, R.P. Moeller, H. Sasabe and J. A. Wilder, Ann. N. Y. Acad. Sci., 279 (1976) 15.
4 M. A. Debolt, A. J. Easteal, P. B. Macedo and C. T. Moynihan, J. Am. Ceram. Soc., 59 (1976) 16.
5 C. T. Moynihan, A. J. Easteal and J. Wilder, J. Phys. Chem., 78 (1974) 2673.
6 G. Teyssedre and C. Lacabanne, J. Phys. D: Appl. Phys., 28 (1995) 1478.
7 G. L. Wilkes, S. Bagrodia, W. Humphries and R. Wildnauer, Polym. Lett. Ed., 13 (1975) 321.
8 G. L. Wilkes, S. Bagrodia, W. Humphries and R. Wildnauer, Polym. Preprints, 16 (1975) 595.
9 G. L. Wilkes, S. Bagrodia, W. Humphries and R. Wildnauer, Polym. Preprints, 16 (1975) 600.
10 G. L. Wilkes and R. Wildnauer, J. Appl. Phys., 46 (1975) 4148.
11 Y. Camberlin, J. P. Pascault, M. Letoffé and P. Claudy, J. Polym. Sci. Polym. Chem. Ed., 20 (1982) 1445.
12 M. J. Abadie and L. Satibi, Eur. Polym. J., 23 (1987) 223.
13 D. Cohen, A. Siegmann and M. Narkis, Polym. Eng. Sci., 27 (1987) 286.
14 S. Monserrat and P. Cortès, Makromol. Chem. Makromol. Symp., 20/21 (1988) 389.
15 C. Bucci, R. Fieschi and G. Guidi, Phys. Rev. Lett., 148 (1966) 816.
16 J. D. Hoffman, G. Williams and E. Passaglia, J. Polym. Sci., C14 (1966) 173.
17 Y. Camberlin, J. Gole, J. P. Pascault, J. P. Durand and F. Dawans, Makromol. Chem., 180 (1979) 2309.
18 M. Xu, W. J. Macknight, C. H. Y. Chen and E. L. Thomas, Polym., 24 (1983) 1327.
19 A. M. North, J. C. Reid and J. B. Shortall, Eur. Polym. J., 5 (1969) 565.
20 A. M. North and J. C. Reid, Eur. Polym. J., 8 (1972) 1129.
21 X. Quan, G. E. Johnson, E. W. Anderson and F. S. Bates, Macrom., 22 (1989) 2451.
22 G. Vigier, J. Tatibouet, A. Benatmane and R. Vassoille, Colloid Polym. Sci., 270 (1992) 1182.
23 C. Lacabanne, A. Lamure, G. Teyssedre, A. Bernes and M. Mourgues, J. of Non Crystal. Sol., 172–174 (1994) 884.
24 L. Cuvé, J. P. Pascault, G. Boiteux and G. Seytre, Polym., 32 (1991) 343.
25 J. C. West and S. L. Cooper, J. Polym. Sci. Symp., 60 (1977) 127.